Suppression of neural fate and control of inner ear morphogenesis by *Tbx1*

Steven Raft[1,*], Sonja Nowotschin[2], Jun Liao[2] and Bernice E. Morrow[2,†]

[1]Department of Neuroscience, Albert Einstein College of Medicine, 1300 Morris Park Avenue, Bronx, NY 10461, USA
[2]Department of Molecular Genetics, Albert Einstein College of Medicine, 1300 Morris Park Avenue, Bronx, NY 10461, USA
*Present address: Department of Cell and Molecular Biology, House Ear Institute, 2100 W 3rd Street, Los Angeles, CA 90057, USA
†Author for correspondence (e-mail: morrow@aecom.yu.edu)

Accepted 22 December 2003

Development 131, 1801-1812
Published by The Company of Biologists 2004
doi:10.1242/dev.01067

Summary

Inner ear sensory organs and VIIIth cranial ganglion neurons of the auditory/vestibular pathway derive from an ectodermal placode that invaginates to form an otocyst. We show that in the mouse otocyst epithelium, *Tbx1* suppresses neurogenin 1-mediated neural fate determination and is required for induction or proper patterning of gene expression related to sensory organ morphogenesis (*Otx1* and *Bmp4*, respectively). *Tbx1* loss-of-function causes dysregulation of neural competence in otocyst regions linked to the formation of either mechanosensory or structural sensory organ epithelia. Subsequently, VIIIth ganglion rudiment form is duplicated posteriorly, while the inner ear is hypoplastic and shows neither a vestibular apparatus nor a coiled cochlear duct. We propose that *Tbx1* acts in the manner of a selector gene to control neural and sensory organ fate specification in the otocyst.

Supplemental data available online

Key words: *Tbx1*, *Ngn1*, *NeuroD*, *Bmp4*, *Otx1*, Otocyst, Neurogenesis, Patterning, Mouse

Introduction

Six inner ear sensory end organs mediate balance and hearing in mammals. Three vestibular canals and associated cristae respond to angular acceleration, while the utricle and saccule with their respective macula respond to gravity and linear acceleration (Goldberg and Hudspeth, 2000). The cochlea and its organ of Corti respond to auditory stimuli (Hudspeth, 2000). Together, these diverse end organs form a closed, continuous epithelium known as the membranous labyrinth. Sensory organs are composed of structural and sensory epithelia (crista, macula, or organ of Corti), the latter tissues comprising a unique arrangement of mechanosensory (hair) and support cells. Afferent innervation of all mechanosensory epithelia is provided by neurons of the VIIIth ganglion, a compound structure with auditory (spiral) and vestibular subdivisions.

Inner ear sensory organs and VIIIth ganglion neurons arise from the otocyst, an epithelial vesicle that forms by invagination of an ectodermal (otic) placode (Kiernan et al., 2002). A subset of otocyst epithelial cells express the *Atonal*-related basic helix-loop-helix (bHLH) genes neurogenin 1 (*Ngn1*) and *NeuroD* (*Neurod1*), delaminate into the mesenchyme, and coalesce with neural crest-derived glial progenitors to form a ganglion (Rubel and Fritzsch, 2002; D'Amico-Martel and Noden, 1983). *Ngn1* is required for neural progenitor determination and formation of the VIIIth ganglion (Ma et al., 1998; Ma et al., 2000), while *NeuroD* requires *Ngn1* activity for its expression and controls delamination and growth factor-mediated neuronal survival (Kim et al., 2001; Liu et al., 2000). Attainment of inner ear morphology by growth/remodeling of the otocyst follows a major period of neurogenesis (Adam et al., 1998). However, during neurogenic stages, homeobox patterning genes such as *Otx1*, *Pax2*, *Dlx5* and *Hmx2/3* are regionally expressed in the otocyst, and their inactivation in mice causes selective loss or malformation of inner ear sensory organs (Morsli et al., 1999; Torres et al., 1996; Merlo et al., 2002; Wang et al., 2001; Wang et al., 1998; Hadrys et al., 1998). Other genes expressed during the period of neurogenesis and implicated in early sensory organ development include bone morphogenetic protein 4 (*Bmp4*) and the Notch signaling modulator lunatic fringe (*Lfng*) (Morsli et al., 1998; Cole et al., 2000).

Divergence of otocyst-derived cell lineages has been modeled as a series of binary fate choices (Fekete and Wu, 2002), however, no single factor or pathway has been identified that differentially influences neural and sensory organ fate specification in vivo. Fate specification in the otocyst could involve compartmentalization (Brigande et al., 2000; Kiernan et al., 1997), change in competence of a pluripotent progenitor field as a function of time (Fritzsch et al., 2002; Cole et al., 2000), or some combination of the two mechanisms.

Tbx1 was identified by sequence homology to the DNA binding domain of *Brachyury* (*T*) (Bollag et al., 1994). *Brachyury*$^{-/-}$ gastrulae generate insufficient mesoderm, and posterior structures are absent at later embryonic stages (Chesley, 1935; Yanagisawa et al., 1981; Herrmann et al., 1990; Wilkinson et al., 1990). Other T-box genes such as *Drosophila optomotor-blind* and mouse *Tbx6* also specify tissue fate and control posteriorization during development (Kopp and Duncan, 1997; Chapman and Papaioannou, 1998). T-box gene mutations cause a variety of human congenital malformations

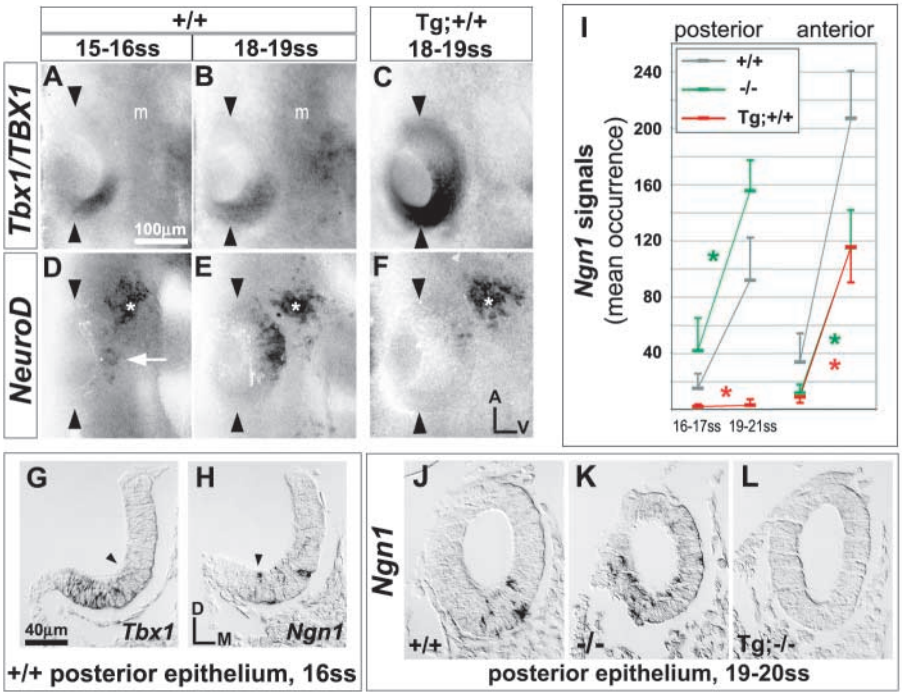

Fig. 1. *Tbx1/TBX1* suppresses expression of neural bHLH genes in the otic placode. (A-F) Lateral surface views of whole mount hybridized embryos. Arrowheads mark the anterior and posterior poles of the invaginating otic placode. a*sterisk*, facial ganglion progenitors; *m*, *Tbx1*-positive mesenchyme. ss, somite stage. (G,H,J-L) Transverse sections (7 μm) through the otic epithelium of whole-mount hybridized embryos. Arrowheads in G and H mark limits of detectable signal; Tg, transgenic. Scale bars in A for A-F and in G for G-L. (I) Quantification of otic epithelial *Ngn1* hybridization signals (perinuclear rings) by serial section analyses for various genotypes at two stages near the onset of neurogenesis (16-17 somites, 19-21 somites; *n*=8-10 epithelia/genotype/stage. **P*<0.01).

(Bamshad et al., 1997; Basson et al., 1997; Li et al., 1997; Braybrook et al., 2001), and *TBX1* haploinsufficiency is implicated in the etiology of Velocardiofacial/DiGeorge syndrome (Merscher et al., 2001; Lindsey et al., 2001). Inner ear and cranial ganglion dysplasias have been described in case reports of this syndrome (Adkins and Gussen, 1974; Black et al.,1975; Ohatni and Schuknecht, 1984), and in mice, *Tbx1* null homozygous mutation causes otocyst hypoplasia and arrest of inner ear morphogenesis (Vitelli et al., 2003; Jerome and Papaioannou, 2001). We have previously reported an occurrence of middle and inner ear abnormalities in adult BAC-transgenic mice expressing *TBX1*, with the inner ear phenotype characterized by dysplastic and ectopic/supernumerary sensory organs (Funke et al., 2001). Here, we show that *Tbx1* suppresses neural fate determination in the otocyst epithelium and is required for proper morphogenesis of inner ear sensory organs.

Materials and methods

Experimental animals

Mice with a targeted disruption of the *Tbx1* locus (Merscher et al., 2001) or with a transgenic insertion (Tg) of BAC 316 DNA (BAC line 316.23) (Funke et al., 2001) were genotyped as previously described and maintained in an FVB background. Wild-type, heterozygous and homozygous mutant embryos were derived from $Tbx1^{+/-} \times Tbx1^{+/-}$ matings; $Tbx1^{+/+}$, $Tbx1^{-/+}$, $Tbx1^{-/-}$, Tg;$Tbx1^{+/+}$, Tg;$Tbx1^{+/-}$ and Tg;$Tbx1^{-/-}$ embryos were derived from either Tg;$^{+/-} \times Tbx1^{+/-}$ matings or Tg;$Tbx1^{+/+} \times Tbx1^{+/+}$ matings. Wild-type morphology and marker expression were also analyzed in CD1 strain (Charles River) embryos; no differences in normal features were discerned between strains. All quantitative comparisons between mutants and wild-type embryos were characterized in the FVB strain. Embryos were staged according to somite number and the method of Theiler (Theiler, 1989).

Immunohistochemistry

Undiluted mAb4D5 (anti-islet1/2) or mAb2H3 (anti-neurofilament, 165kDa) supernatant (Developmental Studies Hybridoma Bank) was applied to tissue sections (for 3 hours at room temperature) and detected with a biotinylated horse anti-mouse IgG conjugate (1:200; Vectalab), avidin-biotin complex formation (Vectalab) and DAB reaction (Research Genetics). Tissue was prepared by Carnoy fixation of whole embryos, which were paraffin wax embedded and serially sectioned at a thickness of 7 μm. Sections were counterstained with either Eosin or Cresyl Violet. Affinity-purified rabbit anti-MATH1 (Helms and Johnson, 1998) was diluted 1:50 in PBS/0.2% Triton X-100/1% goat serum, incubated overnight at 4°C on 4% paraformaldehyde-fixed 12 μm serial cryosections, and detected with a TRITC-conjugated goat anti-rabbit IgG (Jackson Immunoresearch). Double-label immunofluorescence was performed by sequential incubation with anti-MATH1 (anti-Atoh1) and mAb2H3, followed by detection with goat anti-rabbit and goat anti-mouse secondary antibodies conjugated to TRITC and FITC (Jackson Immunoresearch).

Whole-mount in situ hybridization

Digoxigenin-labeled RNA probes for *Tbx1*, *TBX1* (Funke et al., 2001), *Ngn1* (Ma et al., 1998), *NeuroD* (Lee et al., 1995), *Bmp4*, *Lfng* (Morsli et al., 1998), *Gata3* (George et al., 1994), *Fgf3* (Riccomagno, 2002), *Otx1* (*Pst*I/*Sac*I cDNA fragment), and *Pax2* (554 bp coding fragment cloned by PCR) were prepared by standard methods. Whole-mount hybridization and anti-digoxigenin immunochemistry were performed according to the method of Wilkinson (Wilkinson, 1992), with minor modifications. Following enzymatic color development, embryos were post-fixed (3.7% formaldehyde in 0.1 M Mops, pH 7.5), dehydrated, and embedded in paraffin wax for serial sectioning at a thickness of 7 μm. *Bmp4*-, *Lfng*- and *Tbx1*-hybridized embryos were also sunk in 30% sucrose overnight, embedded in OCT compound (Tissue Tek) and cryosectioned at a thickness of 30 μm. Some *Pax2*- and *Gata3*-hybridized embryos were embedded in agarose (3.5%, 8% sucrose, PBS) and vibratome sectioned at a thickness of 40 μm.

Quantitative analyses

Transverse 7 μm serial sections were digitized and imported into either Photoshop7.0 (Adobe) or Openlab3.1.1 (Improvision) at a

resolution of 0.32-0.64 μm/pixel. *NeuroD* and *Ngn1* signal occurrence data were obtained from consecutive serial sections by marking of (perinuclear ring) hybridization signals and automated counting in Photoshop with an Image Processing Toolkit plug-in (Reindeer Graphics). Volumetric data were obtained by integrating traced areas of interest in Openlab3.1.1. Data were tested for significance by multivariate analyses of variance in SAS version 8.1e.

Three-dimensional reconstruction

Serial section sets were aligned using AutoAligner2 software (Bitplane AG). Regions of interest were traced in Photoshop7.0 and reconstructed using Imaris3 software (Bitplane AG).

Results

Tbx1 expression encompasses a subset of presumptive sensory organ territories

Tbx1 expression is regionalized posterolaterally in the early otocyst and anterodorsolaterally, as well, in the later otocyst (Vitelli et al., 2003; Riccomagno et al., 2002; Chapmann et al., 1996). To better characterize its dynamics, otic epithelial *Tbx1* expression was analyzed throughout placode and otocyst stages (E8.5-E12) by RNA hybridization. A diffuse *Tbx1* signal is present posteriorly in the early otic placode (10-12 somites; data not shown). During invagination, a domain border emerges halfway along the placode's anterior-posterior axis (AP midline; Fig. 1A,B) and is maintained through the early otocyst stage (Fig. 2A). Along the medial-lateral axis of the invaginating placode, *Tbx1* signal forms an intensity gradient that falls off medially (Fig. 1G), but by otocyst stages a definitive expression border is present along this axis as well (Fig. S1C,D, http://dev.biologists.org/supplemental/; Fig. 4A). By E10, the *Tbx1* border slopes anterodorsally from the AP midline (Fig. 2B). This border co-localizes with an anterior stripe of *Bmp4* expression (Fig. 3C) and the lateral border of *Lfng/Ngn1/NeuroD* expression, which is complementary to that of *Tbx1* (Fig. 2E, Fig. 3B, Fig. 4B). Between E9.5 and E10, the *Tbx1* domain expands into the posteroventromedial otocyst (Fig. 4A; Fig. S2, http://dev.biologists.org/supplemental/). *Tbx1* signal is absent dorsomedially at all stages (Fig. 1G; Fig. S1A-E, http://dev.biologists.org/supplemental/).

By current fate mapping schemes, E10.5 lateral otocyst regions contributing to the future cristae, utricular macula, and non-sensory cochlea are defined by the expression domains of *Bmp4*, *Lfng* and *Otx1*, respectively (Fekete and Wu, 2002; Morsli et al., 1998). At this stage, *Tbx1* expression encompasses the domains of *Bmp4* and *Otx1*, but is complementary to the lateral portion of the *Lfng/Ngn1/NeuroD* domain (Fig. 3). Signal intensity gradients are observed within the *Tbx1* domain (Fig. 2C, Fig. 3K). Strong *Tbx1* signal is present at all sites of *Bmp4* expression, and graded, low intensity *Tbx1* signal overlaps with *Otx1* signal posteroventrolaterally. By E12, *Tbx1* signal is restricted to the dorsal-most regions of the rudimentary vestibulum – the forming vestibular canals and ampullae – with strong signal selectively marking the latter structures (data not shown) (Vitelli et al., 2003). Thus, *Tbx1* expression in the otocyst epithelium expands in area through E10.5-E11 and thereafter recedes to dorsal vestibular regions.

Complementary expression of *Tbx1* and neural bHLH genes

We next compared *Tbx1* expression with that of the neural bHLH genes *Ngn1* and *NeuroD*, which are expressed sequentially during cranial sensory ganglion development (Ma et al., 1998). *Ngn1* expression is first detected at the onset of invagination (13-14 somites) in a small number of cells located near the AP midline of the placode (data not shown). This is followed by expression of *NeuroD* in the same region; thus, neural determination is initiated near a *Tbx1* expression border (Fig. 1A,D). Epithelial domains of *Ngn1* and *NeuroD* coincide

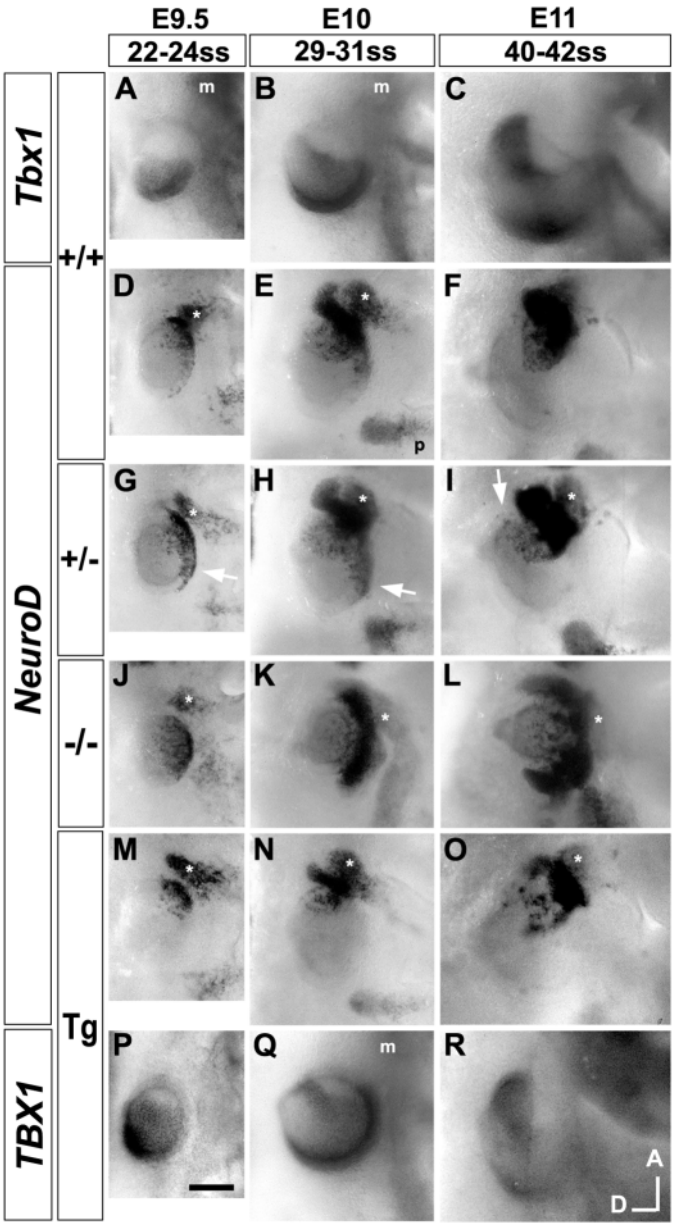

Fig. 2. *Tbx1/TBX1* suppresses *NeuroD* expression in the otocyst. Lateral surface views of whole-mount hybridized embryos arrayed by stage, genotype, and hybridization probe. All transgenic (Tg) embryos shown are of $Tg^{+/+}$ genotype. Mottled otocyst *NeuroD* signals are epithelial; dense signals apposed to the otocyst indicate the VIIIth ganglion. Asterisks mark the facial ganglion. Arrows in G,H,I mark heightened/ectopic *NeuroD* expression in $Tbx1^{+/-}$ otocysts. p, petrosal ganglion. m, *Tbx1*-positive mesenchyme. Scale bar: 100 μm applies to all panels.

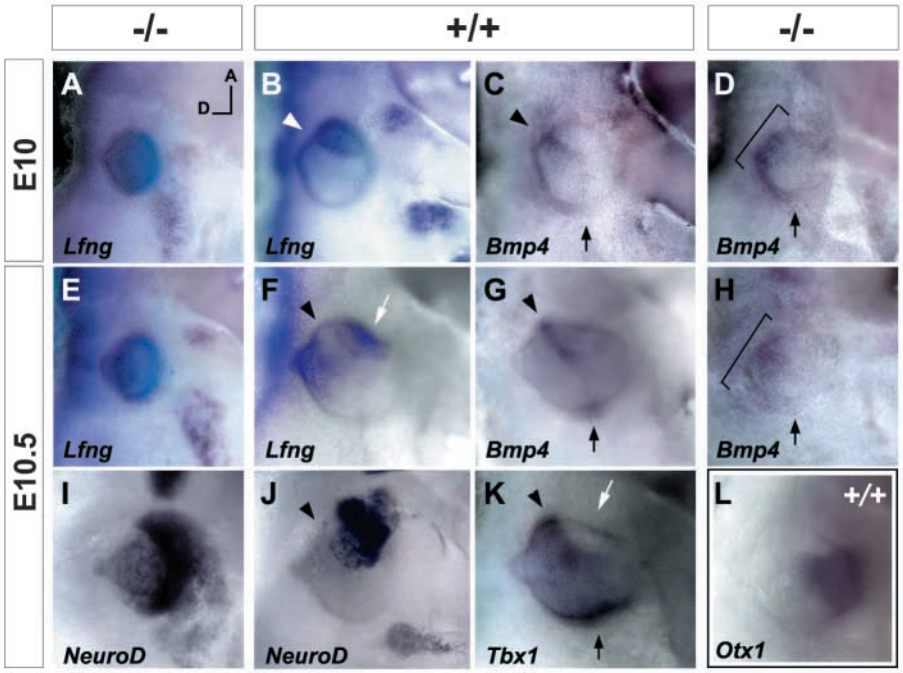

Fig. 3. *Tbx1* patterns *Lfng* and *Bmp4* otocyst expression. Lateral surface views of whole mount hybridized embryos arrayed by stage and genotype. Arrowheads denote position of the *Bmp4* anterior stripe. Black arrows highlight the position of posterior *Bmp4* expression. White arrows mark the anterior region of *Lfng*/neural bHLH gene expression. Brackets in D and H mark the extent of diffuse anterodorsolateral *Bmp4* expression in *Tbx1*$^{-/-}$ otocysts. All images are shown to scale.

through E11.5 (Fig. 4A,B; data not shown). Both expression domains expand into anterolateral, anteroventral and posteroventral portions of the invaginating placode (Fig. 1E,H,J) and overlap with low intensity *Tbx1* signal posteriorly (Fig. 1G,H). By E9.5 a definitive border of *NeuroD* expression emerges at the otocyst AP midline (Fig. 2D), and the posterolateral region remains *Ngn1*/*NeuroD* negative throughout otocyst stages (Fig. 2D-F, Fig. 4B, Fig. 5A). Expression mapping at E9.5 suggests that *NeuroD* and *Tbx1* expression borders are juxtaposed laterally at the AP midline, but overlap in the posteroventral otocyst (Fig. S2, http://dev.biologists.org/supplemental/). At E9.5, all otocyst regions expressing bHLH genes show *NeuroD*-positive cells delaminating from the epithelium (data not shown).

NeuroD and *Ngn1* expression is downregulated in the posteroventral otocyst between E9.5 and E10, a period during which the *Tbx1* domain expands into this region (Fig. 4A,B, Fig. S2, http://dev.biologists.org/supplemental/). Posteroventrally, epithelial *NeuroD* signal decreases 8-fold, while the total anterior value (anterolateral plus anteroventral) increases 2.1-fold (Fig. 5A). By E10, no overlap of *Tbx1* and *NeuroD* expression is detected in the ventral otocyst (Fig. 4A; Fig. S1A-J, Fig. S2, http://dev.biologists.org/supplemental/). In the lateral otocyst between E10 and E11, *NeuroD* and *Tbx1* expression domains remain complementary, even as the shape of their borders change (Fig. 2B,C,E,F, Fig. 3J,K). Between E10 and E11.5, and despite a 2.5-fold increase in otocyst surface area (n=4-6 otocysts), total otocyst *NeuroD* signal (sum of all regions) decreases 2.2-fold (Fig. 5A). In summary, peak expression of neural fate markers occurs at E10, even though downregulation of these genes in the posteroventromedial otocyst begins as early as E9.5. By contrast, expansion of the *Tbx1*-postive otocyst area persists through to at least E10.5, and transient overlap of *Tbx1* and *NeuroD* expression appears to precede downregulation of the latter.

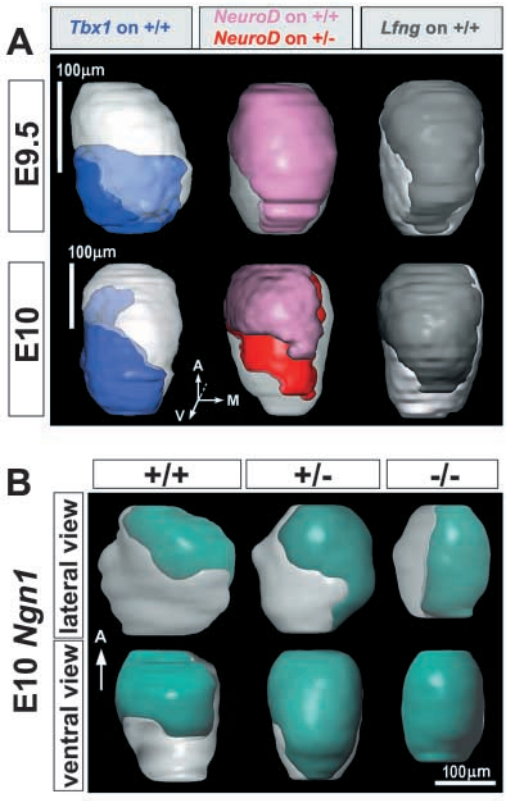

Fig. 4. *Tbx1* determines the position of neural bHLH gene expression domain borders. (A) Expression domain morphologies (colored regions) revealed by 3-D reconstruction of serial section sets. Otocysts are shown in ventral view and rendered transparently to visualize dorsal *Tbx1* expression. Models are normalized for AP length across stages. (B) 3-D reconstructions of the otocyst showing the *Ngn1* expression domain (green) at E10 for each genotype.

Suppression of neural determination in *TBX1* gain-of-function otocysts

To test whether an expanding domain of *Tbx1* activity can suppress otic neurogenesis, *Ngn1* and *NeuroD* expression was analyzed in a transgenic mouse line carrying tandem copies (eight to ten) of human BAC DNA (line 316.23) (Funke et al.,

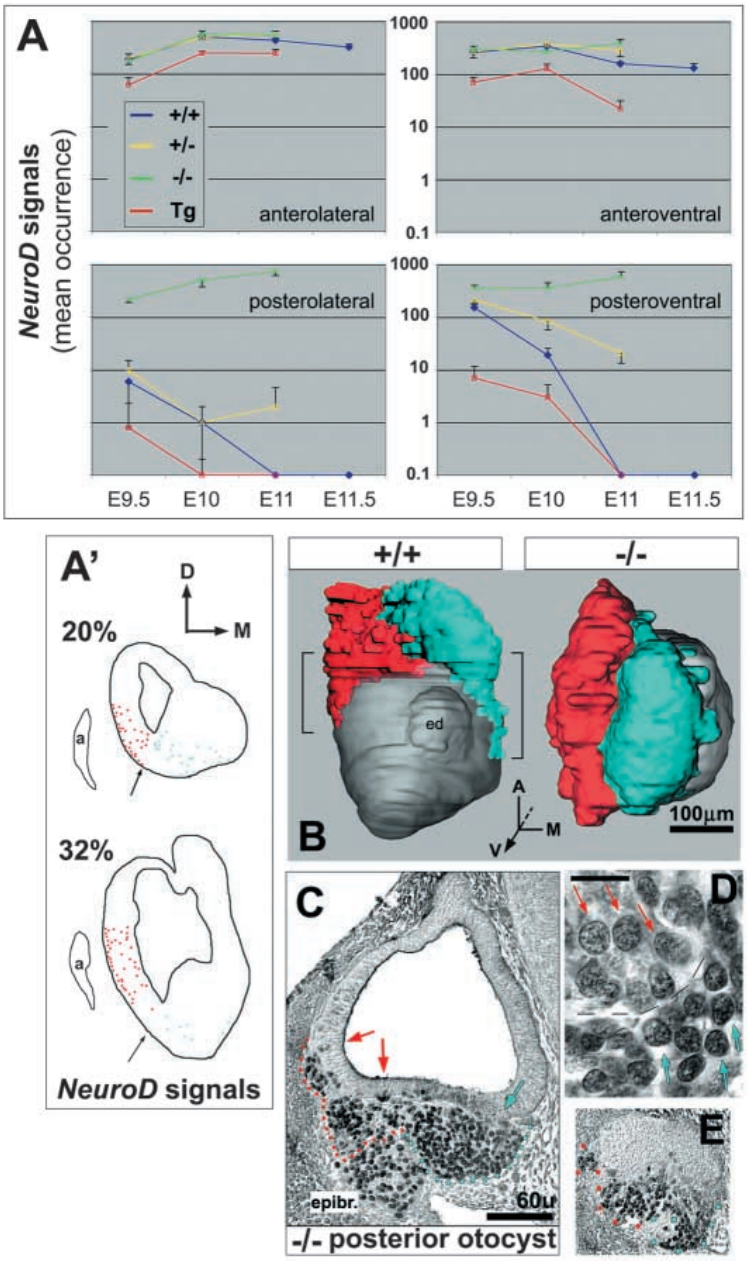

Fig. 5. Ectopic neurogenesis correlates with an expansion of VIIIth ganglion rudiment form. (A) Mean occurrence of epithelial *NeuroD* signals (perinuclear rings) by stage and otocyst region for each of the phenotypes examined, obtained by analyses of serial 7 µm thick transverse sections. Between four and eight right otocysts per genotype per stage were analyzed. Data were normalized to account for differences with wild type in average number of sections when this exceeded 5% (normalization factors: E9.5 Tg, 1.08; E9.5 *Tbx1*$^{-/-}$, 1.09; E10 *Tbx1*$^{-/-}$, 1.22; E11 *Tbx1*$^{-/-}$, 1.53; E11 *Tbx1*$^{+/-}$, 1.09). Transgenic data are for Tg$^{+/+}$, except at E10 (Tg$^{+/-}$). Values are plotted on a log scale, and non-overlapping error bars represent significant differences with $P<0.003$. At later stages these regions are distinguished as shown in A′. (A′) Tracings of E11 wild-type sections at 20 and 32% otocyst (with anterior pole set to zero) showing spatial distributions of *NeuroD*-positive lateral (red in B) and ventral (cyan in B) cells. *a*, anterior cardinal vein. Lateral and ventral regions at stages E9.5 and E10 are distinguished by line VL in Fig. S2, http://dev.biologists.org/supplemental/. (B) 3-D reconstructions of E10.5 otocysts and ganglia (red, lateral subdivision; cyan, ventromedial subdivision), obtained by analyses of sections reacted with mAb4D5 (anti-islet1/2). Brackets demarcate regions of delamination in wild type. Otocysts are rendered transparently. ed, endolymphatic duct outgrowth. Scale bar: 100 µm. (C) Representative section of E10.5 *Tbx1*$^{-/-}$ posterior otocyst reacted with mAb4D5. Arrows highlight sites of cell delamination into the lateral (red) and ventromedial (cyan) pools. epibr., epibranchial ganglion. Scale bar: 60 µm. (D) Lateral (red arrows) and ventromedial (cyan arrows) mAb4D5-positive nuclei in the wild-type E10.5 ganglion. Scale bar: 10 µm. (E) Section through the posterior pole of the E10.5 *Tbx1*$^{-/-}$ otocyst shows delaminating mAb4D5-positive cells.

2001). *TBX1* and flanking genes (5′ and 3′ of *TBX1*) are expressed in transgenic embryos, suggesting the presence and activity of local *TBX1* regulatory elements. Of the four human genes present, only *TBX1* and *PNUTL1* hybridization signals are detected in the transgenic otocyst (Funke et al., 2001). Transgenic embryos hybridized with a species-specific *TBX1* probe show recapitulation of the endogenous *Tbx1* signal together with ectopic signal in the anterior otic placode and otocyst (Fig. 1C, Fig. 2P,Q). *TBX1* transgene and endogenous *Tbx1* otocyst expression patterns are similar at later otocyst stages (Fig. 2C,R). By contrast, *TBX1* signal onset in transgenic mesenchyme is delayed (compare Fig. 1C and B and Fig. 2P and A), affording a period (E9-9.5) during which any gain-of-function effects are probably of epithelial origin.

Ngn1 and *NeuroD* otic epithelial expression is effectively abolished posteriorly and significantly reduced anteriorly in transgenic embryos (Fig. 1F,I,L, Fig. 2M-O, Fig. 5A). The transgene suppresses neurogenesis in *Tbx1*$^{+/+}$, *Tbx1*$^{+/-}$ and *Tbx1*$^{-/-}$ backgrounds (Fig. 1L; data not shown). Transgenic otocysts show differences in neural domain patterning when endogenous gene copy number is varied, but in all instances, *NeuroD* domain borders are shifted anteriorly in the presence of the transgene (Fig. 2N; Fig. S2, http:// dev.biologists.org/ supplemental/). At E10, Tg;*Tbx1*$^{+/-}$ ganglion volume, identified by *NeuroD* signal, is 39% that of wild type ($0.314\pm0.113\times10^6$ vs. $0.798\pm0.206\times10^6$ µm^3; $n=8$ ganglia/class; $P<0.0005$; compare Fig. 2N and E). No qualitative difference with wild type is detected in size of the adjacent facial ganglion rudiment (Fig. 2, asterisks), the neural progenitors of which derive from an epibranchial placode.

Tbx1 loss-of-function causes ectopic neural determination

The generation of a *Tbx1* null mutation by gene targeting has been described (Merscher et al., 2001). The *Tbx1*$^{-/-}$ otocyst is hypoplastic (Fig. 2K,L; Fig. S1P-T, http://dev.biologists.org/ supplemental/), in accordance with previous accounts (Vitelli et al., 2003; Jerome and Papaioannou, 2001), and we find earlier evidence of impaired growth during placode invagination (Fig. 1K). Posteriorly, the invaginating placode of *Tbx1*$^{-/-}$ embryos shows an increase in *Ngn1*/*NeuroD* expression over that in wild type (Fig. 1I,K; data not shown). The *Tbx1*$^{-/-}$ otocyst has a uniform distribution of *Ngn1*/*NeuroD*

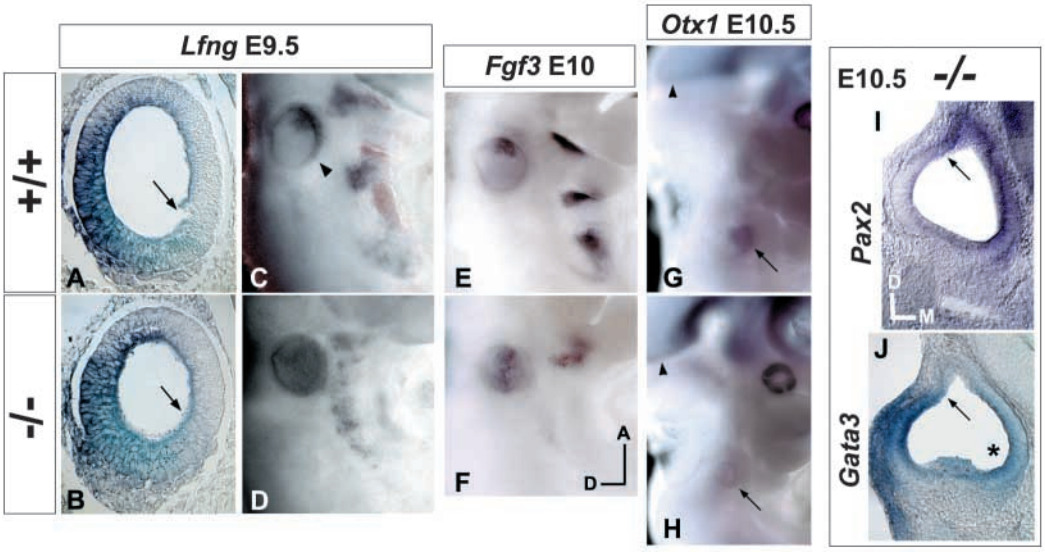

Fig. 6. *Tbx1* is a determinant of otocyst anterior-posterior patterning. (A) 7 μm transverse section through the wild-type anterior otocyst shows a lateral to medial gradient of *Lfng* signal, decreasing medially. Arrow marks the medial extent of detactable signal. Axes are as shown in I. (B) Section, prepared as in A, through the posterior *Tbx1*$^{-/-}$ otocyst. (C-H) Lateral surface views of whole-mount hybridized embryos. Arrowhead in C marks posteroventral *Lfng* signal. Arrowheads in G and H indicate borders of midbrain *Otx1* signal. Arrows indicate the otocyst. (I,J) 40 μm transverse vibratome sections through the anterior otocyst. Arrows indicate common dorsal borders of *Pax2* and *Gata3* signal; asterisk, low intensity ventromedial *Gata3* signal.

expression (laterally and ventrally) along its entire AP length, and no AP midline border forms (Fig. 2J,K,L, Fig. 3I, Fig. 4B, Fig. 5A). Extreme dorsal and medial borders of wild-type *Ngn1*/*NeuroD* expression, together with signal intensity gradients for these markers along the medial-lateral axis, are preserved in *Tbx1*$^{-/-}$ otocysts (Fig. S1F-J,P-T, http://dev.biologists.org/supplemental/).

Tbx1$^{+/-}$ otocysts show a stereotyped pattern of transient ectopic neurogenesis, first posteroventromedially and then anterodorsolaterally (Fig. 2G,H,I, Fig. 4A,B). These loci correspond to sites and times of concerted *Tbx1* expression onset and bHLH gene downregulation described above, suggesting that neurogenic suppression is delayed in the heterozygous state. Ectopic neurogenesis in heterozygotes correlates with increased accumulations of delaminated *NeuroD*-positive cells compared to wild type (Fig. S1K-O, http://dev.biologists.org/supplemental/).

The more persistent and widespread ectopic neurogenesis observed in *Tbx1* null homozygotes correlates with ectopic delamination (Fig. 5C,E) and duplication of VIIIth ganglion rudiment form about the otocyst AP midline (Fig. 2K,L, Fig. 5B). At E10, *Tbx1*$^{-/-}$ ganglion volume, identified by *NeuroD* signal, is 1.83-fold that of wild type ($1.46\pm0.367\times10^6$ vs. $0.798\pm0.206\times10^6$ μm^3; n=8 ganglia/class; P<0.001). By E10.5, anti-islet1/2 (mAb4D5) immunochemistry reveals histodifferentiation of the wild-type ganglion into lateral and ventromedial subdivisions (Fig. S3A,B, http://dev.biologists.org/supplemental/), and islet-positive nuclear size and packing density vary between subdivisions (Fig. 5D; Fig. S3C, http://dev.biologists.org/supplemental/). These features are present along the entire AP length of the E10.5 *Tbx1*$^{-/-}$ ganglion rudiment (Fig. 5C). Evidence of ganglion rudiment splitting near the otocyst AP midline is observed by E11.5 (data not shown), and early labyrinth-stage (E13.5) *Tbx1*$^{-/-}$ ears commonly show a secondary compound ganglion apposed to and innervating the epithelial posterior pole (Fig. 8E,F,G; 4/8 ears auditory and vestibular neuronal cytology; remainder vestibular only). No posterior VIIIth ganglia analyzed possessed a central projection. Anterior to the epithelium, all E13.5 *Tbx1*$^{-/-}$ VIIIth ganglia analyzed (8/8) showed auditory and vestibular neuronal cytology and partial retention of auditory and vestibular ganglion morphology; in addition, all anterior ganglia possessed both peripheral and central projections (Fig. 8A-D). *Tbx1*$^{-/-}$ posterior and anterior VIIIth ganglia are necrotic beyond E14.5 and largely absent by E16.5, suggesting an additional requirement for *Tbx1* in neuronal survival at late embryonic stages.

Tbx1 is a determinant of anterior-posterior otocyst patterning

The foregoing results suggest that *Tbx1* posteriorizes the otocyst by suppressing anterior identity. To test this hypothesis, the distributions of various regional markers were analyzed in *Tbx1*$^{-/-}$ embryos. Early otocyst *Lfng* expression co-localizes with bHLH gene expression and is absent from the *Tbx1*-positive posterolateral region (Fig. 4A; Fig. 6C). In *Tbx1*$^{-/-}$ embryos between E9.5 and E10.5, *Lfng* is ectopically expressed throughout the posterolateral otocyst (Fig. 3A,E; Fig. 6D). A medial-lateral intensity gradient of *Lfng* signal, similar to that present in the wild-type anterior otocyst (decreasing lateral to medial), is present along the entire AP length of the mutant otocyst (Fig. 6A,B). Dorsal and medial border positions of wild-type *Lfng* expression are also preserved in the mutant.

Fibroblast growth factors and their receptors are expressed in the otic epithelium, and FGF signaling functions have been proposed for various stages of inner ear development (Pauley et al., 2003; Pirvola et al., 2002; Pirvola et al., 2000; Mansour

et al., 1993). *Fgf3* is selectively expressed in the anterolateral otocyst (McKay et al., 1996) and defines a portion of the common *Lfng*/bHLH gene domain (Fig. 6E). *Fgf3* expression in E10-10.5 *Tbx1*$^{-/-}$ otocysts is expanded posterolaterally and forms a stripe extending from anterior to posterior poles (Fig. 6F).

Pax2 and *Gata3* expression was assayed to test for effects of *Tbx1* mutation on medial-lateral otocyst patterning. Along this axis, their otocyst expression domains are reciprocal and partially overlapping (Lavoko-Kerali et al., 2002). *Pax2* is expressed medially and is required for genesis of the cochlear duct (Nornes et al., 1990; Torres et al., 1996). *Gata3* hybridization at E10.5 yields a strong lateral signal (Zheng et al., 2003), and the inner ear of *Gata3*$^{-/-}$ mice is severely dysmorphic (Karis et al., 2001). No change was detected in expression patterning of either *Pax2* or *Gata3* in *Tbx1*$^{-/-}$ otocysts between E9.5 and E10.5. Wild-type features of these genes' expression, such as dorsal borders and ventral gradients are preserved in the mutant otocyst (Fig. 6I,J).

Otx1 is expressed in the posteroventrolateral otocyst by E10.25 and loss-of-function results in sensory organ absence (lateral vestibular canal/ampulla) or dysmorphogenesis (lateral crista, maculae, cochlea); no neurogenic phenotype pertaining to the ear has been reported (Fritzsch et al., 2001; Morsli et al., 1999; Acampora et al., 1996). E10.5 and E11 *Tbx1*$^{-/-}$ otocysts lack *Otx1* expression (Fig. 6H) and show ectopic neurogenesis posteroventrolaterally (Fig. 2L, Fig. 3I, Fig. 5A), which persists through to at least E11.5. Thus, *Tbx1* loss-of-function causes anterior (neurogenic) transformation of a posterior otocyst region that contributes to sensory organ development.

Tbx1 is required for proper patterning and maintenance of *Bmp4* expression

To further explore the effects of *Tbx1* activity on sensory organ patterning, *Bmp4* expression was analyzed in *Tbx1*$^{-/-}$ and *Tbx1*$^{+/-}$ embryos. Local antagonism of BMP signaling in the developing chick causes dysmorphogenesis of multiple inner ear sensory organs, with the most severe and frequent defects related to vestibular canal formation (Chang et al., 1999; Gerlach et al., 2000). In the E10.5 mouse otocyst, *Bmp4* hybridization marks the presumptive anterior and lateral cristae (anterior stripe) and posterior crista (Morsli et al., 1998) (Fig. 3G). We have localized the origin of the anterior stripe at E10 to a juxtaposition of *Tbx1* and *Lfng*/neural bHLH gene expression domains (Fig. 2B,E, Fig. 3B,C).

Bmp4 otocyst expression in E10 and E10.5 *Tbx1*$^{-/-}$ embryos is mis-patterned. E10 mutant embryos show a diffuse anterodorsolateral signal in place of an anterior stripe, while an extreme dorsolateral band of signal terminating at the otocyst posterior pole is preserved (Fig. 3D). By E10.5, the wild-type anterior stripe and posterior focus form discrete signals (Fig. 3G), but *Tbx1*$^{-/-}$ otocysts of this stage show a pattern similar to that of E10 mutants (Fig. 3H, Fig. 7D,E). The anterior stripe and posterior focus persist in wild-type otocysts through E11, however, *Tbx1*$^{-/-}$ embryos of this stage showed little to no signal in the otocyst epithelium (Fig. 7F). *Bmp4* otocyst signal in E10 and E10.5 *Tbx1*$^{+/-}$ embryos (15/15) was indistinguishable from wild-type (data not shown). However, all E11 heterozygotes analyzed (four embryos) showed a diffuse anterodorsolateral signal bilaterally in place of an anterior stripe (Fig. 7C), suggesting a requirement for proper *Tbx1* gene dosage in patterning of *Bmp4* otocyst expression.

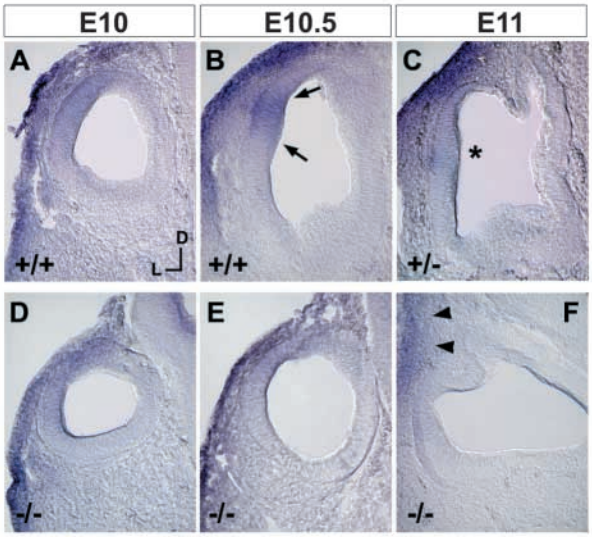

Fig. 7. Otocyst *Bmp4* expression is sensitive to *Tbx1* gene copy number. (A-F) 30 μm transverse cryosections of *Bmp4* hybridized embryos at the level of the anterior stripe (arrows in B). Asterisk in C indicates the absence of a definitive anterior stripe in E11 *Tbx1*$^{+/-}$ otocysts. Arrowheads in F indicate mesenchymal *Bmp4* signal of low intensity compared to wild type.

Tbx1 loss-of-function blocks sensory organ morphogenesis

By E13.5, the six sensory organs of the membranous labyrinth are present in rudimentary form (Morsli et al., 1998). The cochlear duct is partially coiled, saccular and utricular outpouches are conspicuous, and, further dorsally, ampullary swellings are associated with each of the three semicircular canals (Fig. 8E and inset). The non-sensory endolymphatic duct projects dorsally from the medial wall of the labyrinth. At this stage the labyrinth is composed largely of simple or pseudostratified epithelium, however a patch of stratified epithelium that will differentiate into mechanosensory epithelium is associated with each of the developing sensory organs (Sher, 1971). Upper layer cells are innervated by neurites of the VIIIth ganglion (Sher, 1971) and express MATH1 (Chen et al., 2002; Shailam et al., 1999), a bHLH transcription factor that is necessary and sufficient for mechanosensory hair cell differentiation (Bermingham et al., 1999; Zheng and Gao, 2000; Kawamoto et al., 2003).

Identifiable vestibular and auditory sensory organs fail to develop in *Tbx1*$^{-/-}$ embryos (Fig. 8E,I). The E13.5 *Tbx1*$^{-/-}$ inner ear is composed of two ventral chambers – a lateral tube and medial sac – and a dorsal projection, which are continuous and communicate via a narrow duct near the AP midline. Ventral tube and medial sac formation begins with a furrow that runs anteroposteriorly along the ventral wall of the otocyst. The furrow, which is positioned roughly at the otocyst medial-lateral midline and intersects the neurogenic region, deepens and fuses with the dorsal wall of the otocyst (data not shown, but see Fig. 5C). The dorsal projection appears to derive from the endolymphatic projection of the mutant otocyst and

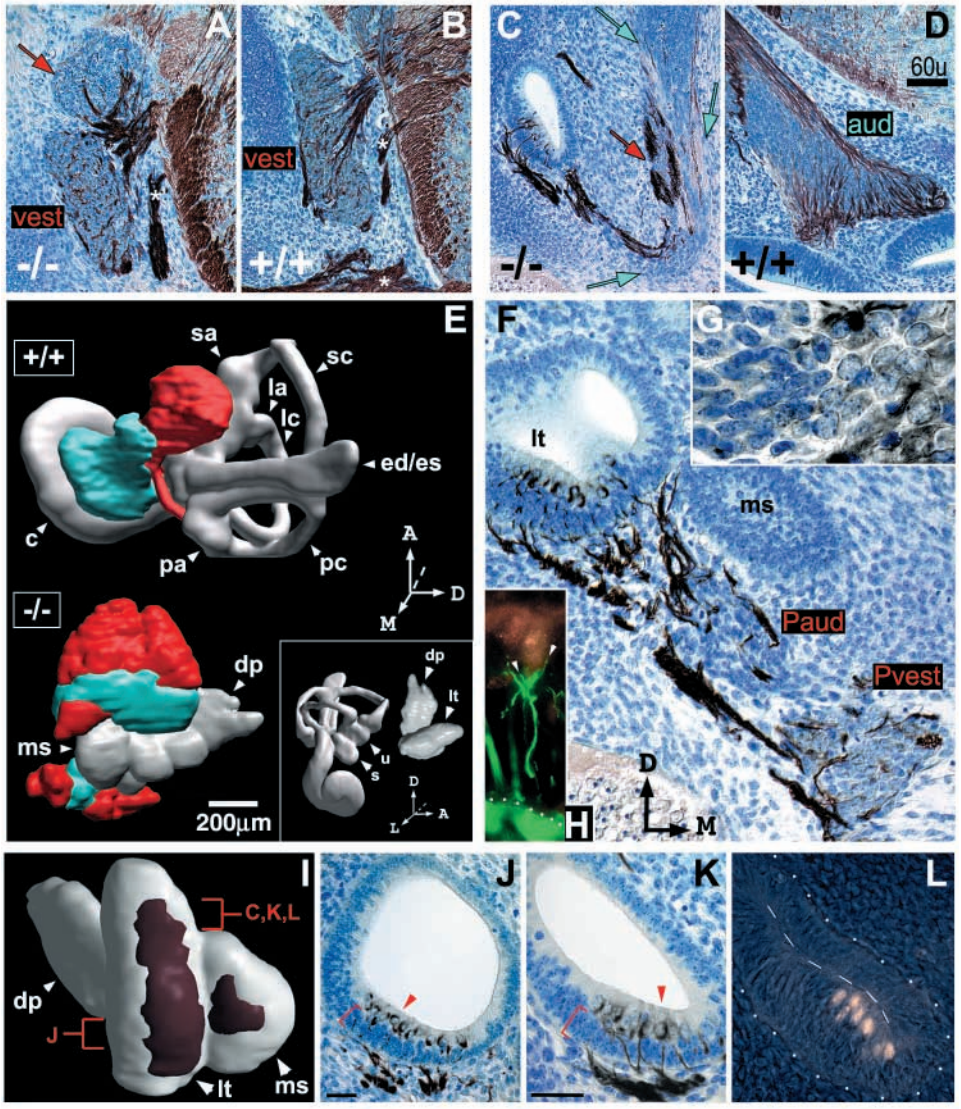

Fig. 8. *Tbx1*$^{-/-}$ inner ear and VIIIth ganglion morphology at E13.5. (A-D,F,G,J,K) Transverse sections through wild-type and *Tbx1*$^{-/-}$ ears/ganglia at E13.5, reacted with mAb2H3 (anti-neurofilament) and counter-stained with Cresyl Violet. Axes in F apply to all except G. Red arrows in A and C indicate regions of vestibular (vest) neuronal cytology and cyan arrows in C auditory (aud) neuronal cytology. The distinguishing cytological features (nuclear size and basophilia) from a mutant posterior ganglion are shown at high magnification in G, with vestibular neuronal cytology shown at right. White asterisks in A and B indicate a branch of the facial nerve. Section shown in F passes through a *Tbx1*$^{-/-}$ posterior compound ganglion and epithelial posterior pole. Pvest, presumptive vestibular ganglion; Paud, presumptive auditory ganglion. Brackets and arrowheads in J and K indicate cellular stratification. Scale bars: in D, 60 μm for A-D; 20 μm for J,K. (E) 3-D reconstructions of serial sections reacted as described above. Presumptive vestibular (red) and auditory (cyan) ganglion tissue is shown in relation to the inner ear epithelium. c, cochlea; sa, superior ampulla; la, lateral ampulla; pa, posterior ampulla; sc, superior canal; lc, lateral canal; pc, posterior canal; ed/es, endolymphatic duct/sac; u, utricle; s, saccule; lt, lateral tube; ms, medial sac; dp, dorsal projection. (H) Double immunolabeling with mAb2H3 and anti-MATH1 shows neurites (in green, arrowheads) enveloping the base of a MATH1-positive cell. Dotted line indicates the basement membrane. (I) Anteroventrolateral view of the *Tbx1*$^{-/-}$ inner ear; the region of stratification and innervation is mapped in brown. Approximate section levels are indicated. (L) MATH1-positive nuclei occupy an apical position in the epithelium. Dashed line indicates the lumen, which is collapsed. Dotted line indicates the basement membrane.

exhibits simple cuboidal epithelial morphology typical of the wild-type endolymphatic duct.

By E13.5, the mutant ventral epithelium, previously a site of neurogenesis, is stratified, innervated, and MATH1 positive (Fig. 8C,F,J,K,L). Neurites of the VIIIth ganglion envelop the base of upper layer MATH1-positive cells (Fig. 8H,J,K), and MATH1 immunoreactivity and innervation patterns are similar across the epithelium (Fig. 8K,L; data not shown). These patterns consist of two patches separated by the cleft between lateral tube and medial sac (Fig. 8I), thus segregation of an initially unitary neural/sensory-competent region may be related to morphogenetic movements of the late otocyst. Lateral patch structure is polarized along the AP axis with respect to the number and morphology of innervated, MATH1-positive cells (Fig. 8J,K,L). Architecture of the medial sac patch is similar to that of the posterior lateral tube.

Discussion

The otocyst has been likened to the *Drosophila* imaginal disc (Fekete, 1996; Brigande et al., 2000). Both are transient embryonic structures derived by invagination of ectoderm and undergo extensive growth and morphogenesis during their maturation. Studies of imaginal disc patterning lead to a three-step model (selector gene action, boundary formation, boundary organizer function) for the transformation of positional information into differentiated structures (Garcia-Bellido et al., 1973; Lawrence and Struhl, 1996; Dahmann and Basler, 1999). Selector genes encoding transcription factors are regionally expressed in primordial epithelia and specify regional identity cell-autonomously and non cell-autonomously. Selector genes mediate compartment boundary formation, a local process involving differential cell affinity and Notch pathway signaling (Milan and Cohen, 2003). For example, *Fng*, a *Drosophila* Notch signaling modulator, is

regulated by the selector gene *apterous* and is critical for boundary formation at the wing imaginal disc (Irvine and Weischaus, 1994; Kim et al., 1995). Boundaries, in turn, secrete long-range signaling molecules of the BMP or WNT families that serve as effectors of global growth and morphogenesis (Nellen et al., 1996; Zecca et al., 1996; Day and Lawrence, 2000).

Tbx1 specifies regional identity and establishes a fate boundary in the otocyst

It is hypothesized that compartment boundaries exist along the three major axes of the otocyst (Fekete, 1996). At the lateral wall of the otocyst, a putative AP midline boundary is defined by anterior expression of *NeuroD*/*Lfng*/*Fgf3* and posterior expression of *Otx1* (Fekete and Wu, 2002). *Otx1* exhibits particular attributes of an otocyst selector gene. Its regional expression encompasses primordia of the non-sensory cochlear duct, lateral canal and lateral crista, and it is required for proper morphogenesis of these end organs and the positioning/segregation of the lateral crista and other proximate sensory epithelia (Morsli et al., 1999; Fritzsch et al., 2001). However, *Otx1* otocyst expression is first detected at E10.25, which precludes a role for this gene in early otocyst patterning.

We find that *Tbx1* expression is localized posterolaterally in the invaginating placode and defines an AP midline expression border prior to otocyst formation. *Tbx1* expression is maintained in the posterolateral otocyst through the time of *Otx1* expression onset. Apart from partial, transient overlap, *Tbx1* and *NeuroD* expression domains are complementary throughout otocyst stages. *TBX1* gain-of-function displaces the *NeuroD* domain border anteriorly. *Tbx1* loss-of-function eliminates AP midline borders of *NeuroD*, *Lfng* and *Fgf3* expression as early as E9.5 and causes ectopic posterolateral expression of all three genes. By contrast, *Otx1* expression is not detected in *Tbx1*$^{-/-}$ otocysts, and the posterolateral otocyst is a site of ectopic neural progenitor delamination between E9.5 and E11.5. At later stages, *Otx1*-dependent sensory organ structures are missing or indistinguishable by morphological criteria. These results suggest that *Tbx1* patterns sensory organ and neural fate assignment in parallel, through local control of regional gene expression (Fig. 9B). *Tbx1* appears to establish a midline boundary between an anterior region of combined neural and sensory epithelial competence and posterior tissue destined to form sensory organ structural components such as the lateral wall of the cochlear duct and lateral canal plate (Fig. 9A). Ectopic expression of *Ngn1* in the *Tbx1*$^{-/-}$ posterolateral otocyst further supports this hypothesis, as *Ngn1* activates *NeuroD* expression and may mediate the selection of neural progenitors from otic epithelium through Notch pathway signaling (Ma et al., 1998).

Otocyst fate boundaries deviate from the major embryonic axes

Initially, the otic placode is symmetrical. Proceeding from a simple model of otocyst compartmentalization, selector gene loss could result in a complete duplication of form about a major axis, and such 'enantiomorphic twin' ear phenotypes have been observed following surgical rotations of the amphibian otic primordium (Harrison, 1936) or perturbation of Hedgehog signaling in zebrafish (Hammond et al., 2003). In *Tbx1*$^{-/-}$ embryos, gene expression patterning and early VIIIth ganglion rudiment form are highly suggestive of anterior otocyst identity duplication in the posterior otocyst. We failed to find an effect of *Tbx1* loss-of-function on a number of early otocyst medial-lateral patterning features, and *Tbx1* may be linked specifically to AP patterning at early otocyst stages. However, the labyrinth-stage *Tbx1*$^{-/-}$ inner ear shows structural variation along its AP axis, and one or more pathways probably mediate inner ear AP patterning in the absence of *Tbx1*. Transplantation studies of avian inner ear primordia provide evidence for a multi-step acquisition of axial polarity (Wu et al., 1998).

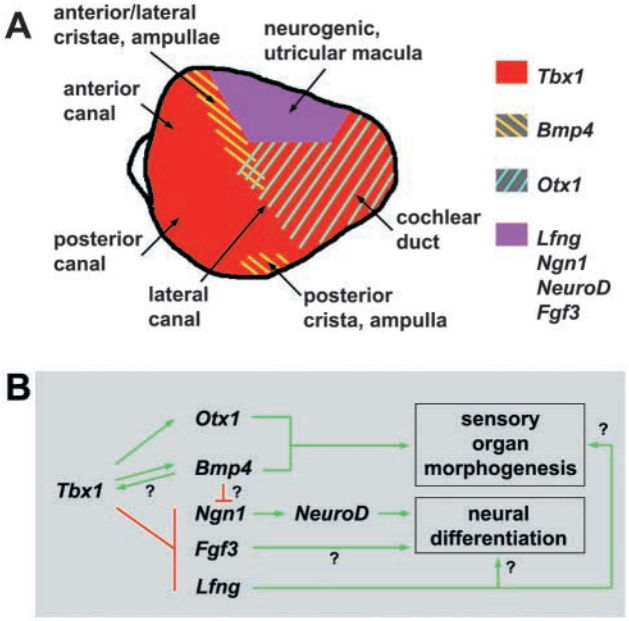

Fig. 9. Summary. (A) Gene expression and predicted fates of the E10.5 otocyst lateral wall. Specification of neural and sensory organ fates appears to involve both reciprocal compartmentalization (*Tbx1/Bmp4/Otx1* vs. bHLH gene expression domain) and change in competence of a pluripotent progenitor field over time (bHLH gene/*Lfng* domain). (B) Neural and particular sensory organ fates may be specified in parallel through opposing actions of *Tbx1* on gene expression. Question marks indicate potential relationships that are unsubstantiated by genetic analyses.

Incomplete symmetry of the *Tbx1*$^{-/-}$ ear about the AP midline may also result from complex and dynamic changes of *Tbx1* expression border morphology during otocyst growth. At E10, the dorsal part of the AP midline border deviates anteriorly from the midline. By E11, it has shifted to a position perpendicular to the AP midline and forms a dorsal-ventral border. During these stages, a stripe of *Bmp4* expression co-localizes with *Tbx1* expression at its interface with the *NeuroD/Lfng* domain border (Fig. 9A). *decapentaplegic* (*dpp*), a *Drosophila* homolog of *Bmp4*, is expressed in a narrow stripe of cells adjacent to the imaginal wing disc AP compartment boundary and encodes a morphogen that controls growth and patterning of the disc (Nellen et al., 1996; Lecuit et al., 1996). The existence of a DPP morphogen gradient is implied by expression of its target genes, one of which is *optomotor-blind*, a T-box gene that controls wing disc regional identity (Podos and Ferguson, 1999). Interestingly, in the otocyst, we find high-intensity *Tbx1* signal at all sites of *Bmp4* expression.

In the mouse, *Bmp4* expression marks sites of developing cristae (Morsli et al., 1998), however the effects of *Bmp4* loss-of-function on inner ear development are unknown because of early embryonic lethality (Winnier et al., 1995). Perturbation of BMP signaling in the chick ear causes a range of sensory organ defects, and vestibular canal morphogenesis is most frequently and severely affected (Chang et al., 1999; Gerlach et al., 2000). *Tbx1*$^{-/-}$ ears lack vestibular canals and it was recently reported that *Tbx1* is required for otocyst *Bmp4* expression (Vitelli et al., 2003). Contrary to this result, we find that *Tbx1*$^{-/-}$ otocysts express *Bmp4* but do not form an anterior stripe and epithelial expression is lost by E11. *Tbx1*$^{+/-}$ otocysts show normal patterning of *Bmp4* through E10.5 and a loss of the anterior stripe by E11. Thus, *Bmp4* patterning appears sensitive to *Tbx1* gene dose in a stage-specific manner. These results, together with the observation of high-intensity *Tbx1* signal at all sites of *Bmp4* expression, suggest that a complex regulatory interaction between *Tbx1* and *Bmp4* is localized to a fate boundary in the anterodorsolateral otocyst (Fig. 9A,B). Studies of comparative expression and epistatic relationships between *Tbx1* and other regulators of *Bmp4* patterning and vestibular canal morphogenesis, such as *Hmx2* (Wang et al., 2001), *Hmx3* (Wang et al., 1998) and *Dlx5* (Merlo et al., 2002) may elucidate cooperative interactions among these genes.

Tbx1 suppresses neurogenesis at some prospective sensory epithelial territories

Evidence of a common progenitor for VIIIth ganglion neurons and mechanosensory cells has been obtained by clonal analyses in chick (Satoh and Fekete, 2003). Furthermore, expression overlap of *Lfng* and neural fate markers in both chick and mouse leads to the suggestion that neural progenitors and utricular and saccular maculae derive from a common anterior otocyst region (Fekete and Wu, 2002; Cole et al., 2000). In the wild-type anterior otocyst, we find overlapping *Ngn1*, *NeuroD*, and *Lfng* expression that is complementary to the *Tbx1* domain (Fig. 9A). Neural bHLH gene expression persists in this region through E11.5, the latest stage assayed for these markers. *Tbx1* loss-of-function has little to no effect on neurogenic activity in this region and does not preclude the subsequent development of anteroventral sensory epithelium. Thus, *Tbx1*-independent pathways probably control neural and sensory epithelial fate assignment at this otocyst region.

The *Lfng*-positive posteroventral otocyst is the presumptive anlage of the organ of Corti (Fekete and Wu, 2002) and initially, this region is *Tbx1*-negative. We show that transient wild-type expression of *Ngn1* and *NeuroD*, together with delamination, precedes the local onset of *Tbx1* expression in this region (see Fig. 4A). Regression of posteroventral neurogenesis is delayed in *Tbx1* heterozygotes, and neurogenesis persists in this region through E11.5 in *Tbx1*$^{-/-}$ otocysts. Conversely, *TBX1* gain of function effectively eliminates posteroventral neurogenesis. Interestingly, *Tbx1* heterozygotes at E11 show delayed regression of neurogenesis at the anterodorsolateral otocyst (see Fig. 2I) and loss of a definitive *Bmp4* anterior stripe. These phenotypes are observed toward the end of a period (E9.75-E11) during which *Tbx1* expression expands into the anterodorsolateral otocyst. Together these results suggest that at some otocyst regions, *Tbx1* regulates the developmental timing by which neural and sensory epithelial competent states are expressed. Functionally, this differs from the effect of *Tbx1* activity at the posterolateral otocyst, where neural competence is fully suppressed at all times and sensory organ structural epithelium is formed.

Conclusion

In this study we have characterized the differential effects of *Tbx1* mutation on neurogenesis and inner ear sensory organ development. *Tbx1* specifies regional identity in the otocyst and is required for the positioning of a fate boundary. Our data support the hypothesis of a relationship between neural and sensory epithelial competence in the otocyst. Furthermore, absence of *Tbx1* causes expression of neural competence in a portion of the otocyst associated with formation of sensory organ structural epithelia. Taken together, our results suggest that *Tbx1* regulates otocyst gene expression locally but affects inner ear growth and morphogenesis in a global manner. *Tbx1* may therefore function as an otocyst selector gene in its control of neurogenesis and sensory organ development. Studies aimed at dissecting the contributions of epithelial and mesenchymal *Tbx1* activity to various aspects of inner ear development using tissue-specific gene inactivation strategies are currently in progress.

In *Xenopus* gastrula ectoderm, BMP signaling suppresses neural competence and induces epidermal fate (Weinstein and Hemmati-Brivanlou, 1999). In the mouse otocyst, the specific effects of *Bmp4* on neural and sensory organ development and its range of action are unknown. Nevertheless, co-localization of *Bmp4* expression and robust ectopic neurogenesis at the *Tbx1*$^{-/-}$ otocyst posterior pole through E10.5 provides a preliminary clue that *Tbx1*-mediated neural suppression may proceed independently of *Bmp4* activity. Finally, the homeobox genes *Eya1* and *Six1* (Xu et al., 1999; Zheng et al., 2003) may function reciprocally to *Tbx1* with respect to neurogenesis, as both are expressed at regions of neural progenitor determination and are required for VIIIth ganglion rudiment formation.

We thank Paula Cohen, Andres Collazo, Andrew Groves, Jean Hebert, Zaven Kaprielian, Doris Wu and two anonymous reviewers for their invaluable commentary. We also thank Jane E. Johnson for a gift of anti-MATH1 antibody, Adam Hartley for suggestions on image analysis, and Haftan Eckhold for assistance with statistical analysis. This work was supported in part by grants from the March of Dimes Foundation #1-FY02-193, American Heart Association Established Investigator Grant, and NIH #1RO1 DC05186-01.

References

Acampora, D., Mazan, S., Avvantaggiato, V., Barone, P., Tuorto, F., Lallemand, Y., Brulet, P. and Simeone, A. (1996). Epilepsy and brain abnormalities in mice lacking the Otx1 gene. *Nat. Genet.* **14**, 218-222.

Adam, J., Myat, A., le Roux, I., Eddison, M., Henrique, D., Ish-Horowicz, D. and Lewis, J. (1998). Cell fate choices and the expression of Notch, Delta, and Serrate homologues in the chick inner ear: parallels with *Drosophila* sense-organ development. *Development* **125**, 4645-4654.

Adkins, W. Y. and Gussen, R. (1974). Temporal bone findings in the third and fourth pharyngeal pouch (DiGeorge) syndrome. *Arch. Otolaryngol.* **100**, 206-208.

Bamshad, M., Lin, R. C., Law, D. J., Watkins, W. C., Krakowiak, P. A., Moore, M. E., Franceschini, P., Lala, R., Holmes, L. B., Gebuhr, T. C. et al. (1997). Mutation in human TBX3 alter limb, apocrine and genital development in ulnar-mammary syndrome. *Nat. Genet.* **16**, 311-315.

Basson, C. T., Bachinsky, D. R., Lin, R. C., Levi, T., Elkins, J. A., Soults, J., Grayzel, D., Kroumpouzou, E., Traill, T. A., Leblanc-Straceski, J. et

al. (1997). Mutations in human TBX5 cause limb and cardiac malformation in Holt-Oram syndrome. *Nat. Genet.* **15**, 30-35.

Bermingham, N. A., Hassan, B. A., Price, S. D., Vollrath, M. A., Nissim, B.-A., Eatock, R. A., Bellen, H. J., Lysakowski, A. and Zoghbi, H. Y. (1999). Math1: An essential gene for the generation of inner ear hair cells. *Science* **284**, 1837-1841.

Black, F. O., Spanier, S. S. and Kohut, R. I. (1975). Aural abnormalities in partial DiGeorge syndrome. *Arch. Otolaryngol.* **101**, 129-134.

Bollag, R. J., Siegfried, Z., Cebra-Thomas, J., Garvey, N., Davidson, E. M. and Silver, L. M. (1994). An ancient family of embryonically expressed mouse genes sharing a conserved protein motif with the T locus. *Nat. Genet.* **7**, 383-389.

Braybrook, C., Doudney, K., Marcano, A. C., Arnason, A., Bjornsson, A., Patton, M. A., Goodfellow, P. J., Moore, G. E. and Stanier, P. (2001). The T-box transcription factor gene TBX22 is mutated in X-linked cleft palate and ankyloglossia. *Nat. Genet.* **29**, 179-183.

Brigande, J. V., Kiernan, A. E., Gao, X., Iten, L. E. and Fekete, D. M. (2000). Molecular genetics of pattern formation in the inner ear: Do compartment boundaries play a role? *Proc. Natl. Acad. Sci. USA* **97**, 11700-11706.

Chang, W., Nunes, F., de Jesus-Escobar, J. M., Harland, R. M. and Wu, D. K. (1999). Ectopic noggin blocks sensory and nonsensory organ morphogenesis in the chicken inner ear. *Dev. Biol.* **216**, 369-381.

Chapman, D. L., Garvey, N., Hancock, S., Alexiou, M., Agulnik, S. I., Gibson-Brown, J. J., Cebra-Thomas, J., Bollag, R. J., Silver, L. M. and Papaioannou, V. E. (1996). Expression of the T-box family genes, Tbx1-Tbx5, during early mouse development. *Dev. Dyn.* **206**, 379-390.

Chapman, D. L. and Papaioannou, V. E. (1998). Three neural tubes in mouse embryos with mutations in the T-box gene Tbx6. *Nature* **391**, 695-697.

Chen, P., Johnson, J. E., Zoghbi, H. Y. and Segil, N. (2002). The role of Math1 in inner ear development: uncoupling the establishment of the sensory primordium from hair cell fate determination. *Development* **129**, 2495-2505.

Chesley, P. (1935). Development of the short-tailed mutation in the house mouse. *J. Exp. Zool.* **29**, 437-438.

Cole, L. K., le Roux, I., Nunes, F., Laufer, E., Lewis, J. and Wu, D. K. (2000). Sensory organ generation in the chicken inner ear: contributions of Bone Morphogenetic Protein 4, Serrate1, and Lunatic Fringe. *J. Comp. Neurol.* **424**, 509-520.

D'Amico-Martel, A. and Noden, D. M. (1983). Contributions of placodal and neural crest cells to avian cranial peripheral ganglia. *Am. J. Anat.* **166**, 445-468.

Dahmann, C. and Basler, K. (1999). Compartment boundaries at the edge of development. *Trends Genet.* **15**, 320-326.

Day, S. J. and Lawrence, P. A. (2000). Measuring dimensions: the regulation of size and shape. *Development* **127**, 2977-2987.

Fekete, D. M. (1996). Cell fate specification in the inner ear. *Curr. Opin. Neurobiol.* **6**, 533-541.

Fekete, D. M. and Wu, D. K. (2002). Revisiting cell fate specification in the inner ear. *Curr. Opin. Neurobiol.* **12**, 35-42.

Fritzsch, B., Beisel, K. W., Jones, K., Farinas, I., Maklad, A., Lee, J. and Reichardt, L. F. (2002). Development and evolution of inner ear sensory epithelia and their innervation. *J. Neurobiol.* **53**, 143-156.

Fritzsch, B., Signore, M. and Simeone, A. (2001). Otx1 null mutant mice show partial segregation of sensory epithelia comparable to lamprey ears. *Dev. Genes Evol.* **211**, 388-396.

Funke, B., Epstein, J. A., Kochilas, L. K., Lu, M. M., Pandita, R. K., Liao, J., Bauerndistel, R., Schuler, T., Schorle, H., Brown, M. C. et al. (2001). Mice overexpressing genes from the 22q11 region deleted in velo-cardio-facial syndrome/DiGeorge syndrome have middle and inner ear defects. *Hum. Mol. Genet.* **10**, 2549-2556.

Garcia-Bellido, A., Ripoll, P. and Morata, G. (1973). Developmental compartmentalization of the wing disk of Drosophila. *Nature* **245**, 251-253.

George, K. M., Leonard, M. W., Roth, M. E., Lieuw, K. H., Kioussis, D., Grosveld, F. and Engel, J. D. (1994). Embryonic expression and cloning of the murine GATA-3 gene. *Development* **120**, 2673-2686.

Gerlach, L. M., Hutson, M. R., Germiller, J. A., Nguyen-Luu, D., Victor, J. C. and Barald, K. F. (2000). Addition of the BMP4 antagonist, noggin, disrupts avian inner ear development. *Development* **127**, 45-54.

Goldberg, M. E. and Hudspeth, A. J. (2000). The vestibular system. In *Principles of Neural Science* (ed. E. R. Kandel, J. H. Schwartz and T. M. Jessell), pp. 801-815. New York: McGraw-Hill.

Hadrys, T., Braun, T., Rinkwitz-Brandt, S., Arnold, H. H. and Bober, E. (1998). Nkx5-1 controls semicircular canal formation in the mouse inner ear. *Development* **125**, 33-39.

Hammond, K. L., Loynes, H. E., Folarin, A. A., Smith, J. and Whitfield, T. T. (2003). Hedgehog signaling is required for correct anteroposterior patterning of the zebrafish otic vesicle. *Development* **130**, 1403-1417.

Helms, A. W. and Johnson, J. E. (1998). Progenitors of dorsal commissural interneurons are defined by MATH1 expression. *Development* **125**, 919-928.

Harrison, R. G. (1936). Relations of symmetry in the developing ear of Amblystoma punctatum. *Proc. Natl. Acad. Sci. USA* **22**, 238-247.

Herrmann, B. G., Labeit, S., Pustka, A., King, T. R. and Lehrach, H. (1990). Cloning of the T gene required in mesoderm formation in the mouse. *Nature* **343**, 617-622.

Hudspeth, A. J. (2000). Hearing. In *Principles of Neural Science* (ed. E. R. Kandel, J. H. Schwartz and T. M. Jessell), pp. 801-815. New York: McGraw-Hill.

Irvine, K. D. and Wieschaus, E. (1994). fringe, a boundary-specific signaling molecule, mediates interactions between dorsal and ventral cells during Drosophila wing development. *Cell* **79**, 595-606.

Jerome, L. A. and Papaioannou, V. E. (2001). DiGeorge syndrome phenotype in mice mutant for the T-box gene, Tbx1. *Nat. Genet.* **27**, 286-291.

Karis, A., Pata, I., Hikke van Doorninck, J., Grosveld, F., de Zeeuw, C. I., de Caprona, D. and Fritzsch, B. (2001). Transcription factor GATA-3 alters pathway selection of olivocochlear neurons and affects morphogenesis of the inner ear. *J. Comp. Neurol.* **429**, 615-630.

Kawamoto, K., Ishimoto, S.-I., Minoda, R., Brough, D. E. and Raphael, Y. (2003). Math1 gene transfer generates new cochlear hair cells in mature guinea pigs in vivo. *J. Neurosci.* **23**, 4395-4400.

Kiernan, A. E., Nunes, F., Wu, D. K. and Fekete, D. M. (1997). The expression domain of two related homeobox genes defines a compartment in the chicken inner ear that may be involved in semicircular canal formation. *Dev. Biol.* **191**, 215-229.

Kiernan, A. E., Steele, K. P. and Fekete, D. M. (2002). Development of the mouse inner ear. In *Mouse development* (ed. J. Rossant and P. Tam), pp. 539-566. San Diego: Academic Press.

Kim, J., Irvine, K. D. and Carroll, S. B. (1995). Cell recognition, signal induction, and symmetrical gene activation at the dorsal-ventral boundary of the developing Drosophila wing. *Cell* **82**, 795-802.

Kim, W.-Y., Fritzsch, B., Serls, A., Bakel, L. A., Huang, E. J., Reichardt, L. F., Barth, D. S. and Lee, J. E. (2001). NeuroD-null mice are deaf due to a severe loss of the inner ear sensory neurons during development. *Development* **128**, 417-426.

Kopp, A. and Duncan, I. (1997). Control of cell fate and polarity in the adult abdominal segments of *Drosophila* by optomotor-blind. *Development* **124**, 3715-3726.

Lavoko-Kerali, G., Rivolta, M. N. and Holley, M. (2002). Expression of the transcription factors GATA3 and Pax2 during development of the mammalian inner ear. *J. Comp. Neurol.* **442**, 378-391.

Lawrence, P. A. and Struhl, G. (1996). Morphogens, compartments, and pattern: Lessons from Drosophila? *Cell* **85**, 951-961.

Lecuit, T., Brook, W. J., Ng, M., Calleja, M., Sun, H. and Cohen, S. M. (1996). Two distinct mechanisms for long-range patterning by Decapentaplegic in the Drosophila wing. *Nature* **381**, 387-393.

Lee, J. E., Hollenberg, S. M., Snider, L., Turner, D. L., Lipnick, N. and Wientraub, H. (1995). Conversion of Xenopus ectoderm into neurons by NeuroD, a basic helix-loop-helix protein. *Science* **268**, 836-844.

Li, Q. Y., Newbury-Ecob, R. A., Terrett, J. A., Wilson, D. I., Curtis, A. R., Yi, C. H., Gebuhr, T., Bullen, P. J., Robson, S. C., Strachan, T. et al. (1997). Holt-Oram syndrome is caused by mutation in TBX5, a member of the Brachyury (T) gene family. *Nat. Genet.* **15**, 21-29.

Lindsay, E. A., Vitelli, F., Su, H., Morishima, M., Huynh, T., Pramparo, T., Jurecic, V., Ogunrinu, G., Sutherland, H. F., Scambler, P. J. et al. (2001). Tbx1 haploinsufficiency in the DiGeorge syndrome region causes aortic arch defects in mice. *Nature* **410**, 97-101.

Liu, M., Pereira, F. A., Price, S. D., Chu, M.-J., Shope, C., Himes, D., Eatock, R. A., Brownell, W. E., Lysakowski, A. and Tsai, M.-J. (2000). Essential role of BETA2/NeuroD1 in development of the vestibular and auditory systems. *Genes Dev.* **14**, 2839-2854.

Ma, Q., Anderson, D. J. and Fritzsch, B. (2000). Neurogenin1 null mutant ears develop fewer, morphologically normal hair cells in smaller sensory epithelia devoid of innervation. *JARO* **1**, 129-143.

Ma, Q., Chen, Z., del Barco Barantes, I., de la Ponpa, J. L. and Anderson, D. J. (1998). neurogenin1 is essential for the determination of neuronal precursors for proximal cranial sensory ganglia. *Neuron* **20**, 469-482.

Mansour, S. L., Goddard, J. M. and Capecchi, M. R. (1993). Mice homozygous for a targeted disruption of the proto-oncogene int-2 have developmental defects in the tail and inner ear. *Development* **117**, 13-28.

McKay, I., Lewis, J. and Lumsden, A. (1996). The role of FGF-3 in early inner ear development: an analysis in normal and kreisler mutant mice. *Dev. Biol.* **174**, 370-378.

Merlo, G. R., Paleari, L., Mantero, S., Zerega, B., Adamska, M., Rinkwitz, S., Bober, E. and Levi, G. (2002). The Dlx5 homeobox gene is essential for vestibular morphogenesis in the mouse embryo through a BMP4-mediated pathway. *Dev. Biol.* **248**, 157-169.

Merscher, S., Funke, B., Epstein, J. A., Heyer, J., Anne, P., Lu, M. M., Xavier, R., Demay, M. B., Russell, R. G., Factor, S. et al. (2001). TBX1 is responsible for cardiovascular defects in velo-cardio-facial/DiGeorge syndrome. *Cell* **104**, 619-629.

Milan, M. and Cohen, S. M. (2003). A re-evaluation of the contributions of Apterous and Notch to the dorsoventral lineage restriction boundary in the Drosophila wing. *Development* **130**, 553-562.

Morsli, H., Choo, D., Ryan, A., Johnson, R. and Wu, D. K. (1998). Development of the mouse inner ear and origin of its sensory organs. *J. Neurosci.* **18**, 3327-3335.

Morsli, H., Tuorto, F., Choo, D., Pia Postiglione, M., Simeone, A. and Wu, D. K. (1999). Otx1 and Otx2 activities are required for the normal development of the mouse inner ear. *Development* **126**, 2335-2343.

Nellen, D., Burke, R., Struhl, G. and Basler, K. (1996). Direct and long-range action of a DPP morphogen gradient. *Cell* **85**, 357-368.

Nornes, H. O., Dressler, G. R., Knapik, E. W., Deutsch, U. and Gruss, P. (1990). Spatially and temporally restricted expression of Pax2 during murine neurogenesis. *Development* **109**, 797-809.

Ohtani, I. and Schuknecht, H. F. (1984). Temporal bone pathology in DiGeorge's syndrome. *Ann. Otol. Rhinol. Laryngol.* **93**, 220-224.

Pauley, S., Wright, T. J., Pirvola, U., Ornitz, D., Beisel, K. W. and Fritzsch, B. (2003). Expression and function of FGF10 in mammalian inner ear development. *Dev. Dyn.* **227**, 203-215.

Pirvola, U., Spencer-Dene, B., Xing-Qun, L., Kettunen, P., Thesleff, I., Fritzsch, B., Dickson, C. and Ylikoski, J. (2000). FGF/FGFR-2(IIIb) signaling is essential for inner ear morphogenesis. *J. Neurosci.* **20**, 6125-6134.

Pirvola, U., Ylikoski, J., Trokovic, R., Hebert, J., McConnell, S. and Partanen, J. (2002). FGFR1 is required for the development of the auditory sensory epithelium. *Neuron* **35**, 671-680.

Podos, S. D. and Ferguson, E. L. (1999). Morphogen gradients: new insights from DPP. *Trends Genet.* **15**, 396-402.

Riccomagno, M. M., Martinu, L., Mulheisen, M., Wu, D. K. and Epstein, D. J. (2002). Specification of the mammalian cochlea is dependent on Sonic hedgehog. *Genes Dev.* **16**, 2365-2378.

Rubel, E. W. and Fritzsch, B. (2002). Auditory system development: primary auditory neurons and their targets. *Annu. Rev. Neurosci.* **25**, 51-101.

Satoh, T. and Fekete, D. M. (2003). Mechanosensory epithelial cells and ganglion cells are clonally related. *Assoc. Res. Otolaryngol.* **23** (Abstr. No. 1776).

Shailam, R., Lanford, P. J., Dolinsky, C. M., Norton, C. R., Gridley, T. and Kelly, M. W. (1999). Expression of proneural and neurogenic genes in the embryonic mammalian vestibular system. *J. Neurocytol.* **28**, 809-819.

Sher, A. E. (1971). The embryonic and postnatal development of the inner ear of the mouse. *Acta Otolaryngologica*, **Suppl. 285**, 5-77.

Theiler, K. (1989). *The House Mouse: Atlas of Embryonic Development.* New York: Springer.

Torres, M., Gomez-Pardo, E. and Gruss, P. (1996). Pax2 contributes to inner ear patterning and optic nerve trajectory. *Development* **122**, 3381-3391.

Vitelli, F., Viola, A., Morishima, M., Pramparo, T., Baldini, A. and Lindsay, E. A. (2003). TBX1 is required for inner ear morphogenesis. *Hum. Mol. Genet.* **12**, 2041-2048.

Wang, W., Chan, E. K., Baron, S., van de Water, T. R. and Lufkin, T. (2001). Hmx2 homeobox gene control of murine vestibular morphogenesis. *Development* **128**, 5017-5029.

Wang, W., van de Water, T. R. and Lufkin, T. (1998). Inner ear and maternal reproductive defects in mice lacking the Hmx3 homeobox gene. *Development* **125**, 621-634.

Weinstein, D. C. and Hemmati-Brivanlou, A. (1999). Neural induction. *Annu. Rev. Cell Dev. Biol* **15**, 411-433.

Wilkinson, D. G. (1992). *In Situ Hybridization: A Practical Approach.* Oxford: IRL Press.

Wilkinson, D. G., Bhatt, S. and Herrmann, B. G. (1990). Expression pattern of the mouse T gene required in mesoderm formation in the mouse. *Nature* **343**, 617-622.

Winnier, G., Blessing, M., Labosky, P. A. and Hogan, B. L. M. (1995). Bone morphogenetic protein-4 is required for mesoderm formation and patterning in the mouse. *Genes Dev.* **9**, 2105-2116.

Wu, D. K., Nunes, F. D. and Choo, D. (1998). Axial specification for sensory organs versus non-sensory structures of the chicken inner ear. *Development* **125**, 11-20.

Xu, P.-X., Adams, J., Peters, H., Brown, M. C., Heaney, S. and Maas, R. (1999). Eya1-deficient mice lack ears and kidneys and show abnormal apoptosis of organ primordia. *Nat. Genet.* **23**, 113-117.

Yanagisawa, K. O., Fujimoto, H. and Urushihara, H. (1981). Effects of the Brachyury (T) mutation on morphogenetic movement in the mouse embryo. *Dev. Biol.* **87**, 242-248.

Zecca, M., Basler, K. and Struhl, G. (1996). Direct and long-range action of a wingless morphogen gradient. *Cell* **87**, 833-844.

Zheng, J. L. and Gao, W.-Q. (2000). Overexpression of Math1 induces robust production of extra hair cells in postnatal rat inner ears. *Nat. Neurosci.* **3**, 580-586.

Zheng, W., Huang, L., Zhu-Bo, W., Silvius, D., Tang, B. and Xu, P.-X. (2003). The role of Six1 in mammalian auditory system development. *Development* **130**, 3989-4000.